Rotordynamics of a Mechanical Face Seal Riding on a Flexible Shaft

An Sung Lee

Itzhak Green

Woodruff School of Mechanical Engineering,
Georgia Institute of Technology,
Atlanta, GA 30332

A mechanical face seal is a triboelement intended to minimize leakage between a rotating shaft and a housing, while allowing the shaft to rotate as freely as possible. All dynamic analysis to date have concentrated on the seal itself. In reality, however, especially in high speed turbomachinery, shafts are made flexible and the dynamics of seals must be coupled with the dynamics of shafts. (Perhaps the dynamics of other triboelements, such as gears, bearings, etc., have to be included as well.) In this work the complex extended transfer matrix method is established to solve for the steady state response of a noncontacting flexibly mounted rotor mechanical face seal that rides on a flexible shaft. This method offers a complete dynamic analysis of a seal tribosystem, including effects of shaft inertia and slenderness, fluid film, secondary seal, flexibly mounted rotating element, and axial offset of the rotor center of mass. The results are then compared to those obtained from an analysis that implicitly assumed the shaft rigid. The comparison shows that shaft dynamics can greatly affect the seal performance even at relatively low speeds.

Introduction

Modern high performance turbomachinery operate under extreme conditions such as high speeds, high pressures, high temperatures, and possibly hazardous environments. Mechanical face seals have experienced a rapid growth in such applications, specifically in cooling pumps of nuclear power plants, jet engine compressors, and pumps handling liquified petroleum gases. To ensure long life and reliable operation seals must be inherently stable, and their steady-state behavior should be such that wear and leakage are minimum. Mechanical face seal dynamics has been an active area of research in the past three decades as extensively reviewed by Etsion (1982, 1985, and 1991). Additional work by Salant and Blasbalg (1991), and Yasuna and Hughes (1992) investigated the dynamics of two-phase seals limited to one axial degree of freedom. Without exception, however, all research to date on the dynamic behavior of mechanical seals concentrated on the seal itself, disregarding the effects that the rotating shaft might have on the seal. Noteworthy is Marcscher's (1987) discussion on the damage caused by shaft vibration to internal components in centrifugal pumps, such as bearings, mechanical seals, etc. In reality, especially in high speed turbomachinery, shafts cannot be considered rigid a priori and the dynamic behavior of the triboelements (in this work, a mechanical face seal) must be coupled with the dynamics of the shaft.

Recently Green (1989 and 1990) provided a closed-form solution for the dynamic behavior of a flexibly mounted rotor (FMR) mechanical face seal. The rotor is free to move axially, tilt (nutation), and whirl about the shaft axis of rotation. That work also did not include shaft dynamics. However, the equations of motion for the rotor derived there will be useful herein. In this work the complex extended transfer matrix will be formulated to solve, for the first time, the coupled problem of the dynamics of a flexible shaft and a noncontacting FMR mechanical face seal that rides on it.

The transfer matrix method (originated with the works of Myklestad (1944) and Prohl (1945)) is well-suited to handle shaft dynamics problems (Pestel and Leckie, 1963, and Rao, 1983). To apply this method to a shaft-seal tribosystem the support and fluid-film rotordynamic coefficients of the seal (Green and Etsion, 1985, and Green, 1987, respectively) must be reproduced in a complex extended transfer matrix form. As a practical example the method will be applied to analyze a test rig which was built to experimentally investigate the dynamic behavior of a noncontacting FMR mechanical face seal (Lee and Green, 1992). The rotor response to its own initial misalignment as measured with respect to the axis of rotation, the effects of the axial offset of the rotor center of mass from the pitch axis, and the shaft slenderness will be investigated. Since the complex extended transfer matrix method is modular it can accommodate other triboelements such as bearings, gears, and the like, to provide a comprehensive dynamic investigation of detailed tribosystems.

The Test Rig

To establish the complex extended transfer method (CETM) only a schematic model of the FMR face seal test rig is necessary (Fig. 1). In the rig the shaft is cantilevered to a precision spindle driven by an electric a motor. (The cantilevered configuration

Contributed by the Tribology Division of THE AMERICAN SOCIETY OF MECHANICAL ENGINEERS and presented at the STLE/ASME Tribology Conference, New Orleans, La., October 24–27, 1993. Manuscript received by the Tribology Division February 1, 1993. Paper No. 93-Trib-8. Associate Technical Editor: I. Etsion.

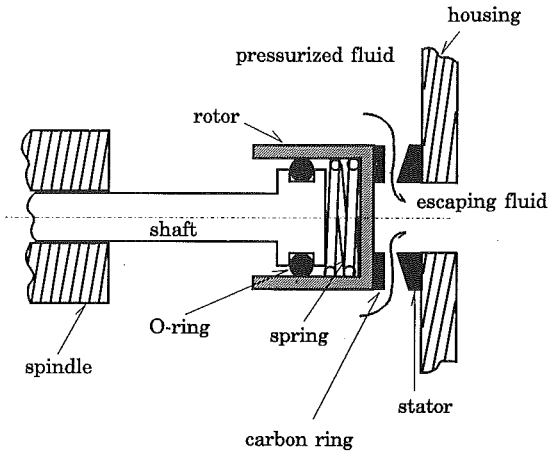

Fig. 1 Schematic model of a noncontacting FMR seal test rig

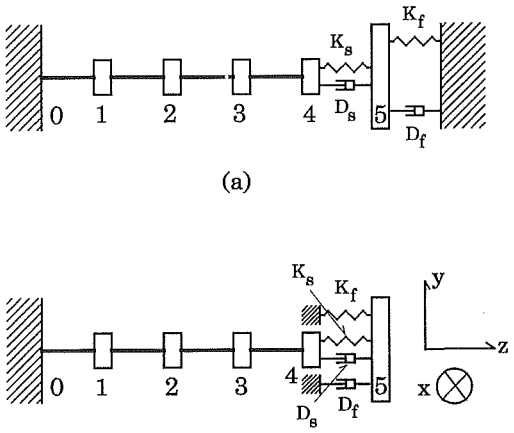

Fig. 2 Lumped parameter models of the seal test rig

affects only the boundary conditions, but not the method.) The rotor is flexibly mounted on the shaft by means of an elastomeric Nitrile (Buna N) O-ring and a spring. The flat-face carbon ring (primary seal) is attached to the rotor as it rotates facing the coned-face stator (stainless steel mating ring). The fluid leaks through the sealing dam in the direction of a negative pressure gradient. The pressure in the sealing dam separates the carbon ring and the stator and provides the rotor with fluid film stiffness, whereas fluid viscosity provides the damping. More technical information on the test rig can be found in Lee and Green (1992).

System Modeling

For the purpose of solving the system dynamics the test rig is modeled in Fig. 2(*a*) by five lumped disks having transnational and rotatory inertias. K_f, K_s, D_f, and D_s, represent coefficients in the angular mode. The equivalent model (in Fig. 2(*b*)) emphasizes the free end boundary conditions of zero moment and shear force. The rotor (disk 5) is subjected to two forcing inputs: The first is the fixed stator misalignment, γ_s, and the second is the initial rotor misalignment, γ_{ri}. Both are measured with respect to the axis of shaft rotation. The equations of motion of an FMR face seal in the inertial *xyz*-system are (Green, 1990)

$$I_t\ddot{\gamma}_x + I_p\omega\dot{\gamma}_y + (D_s + D_f)\dot{\gamma}_x + \left(D_s + \frac{1}{2}D_f\right)\omega\gamma_y + (K_s + K_f)\gamma_x = \gamma_s\left(K_f \cos\psi_s + \frac{1}{2}D_f\omega \sin\psi_s\right) + K_s\gamma_{ri}\cos\omega t$$

$$I_t\ddot{\gamma}_y - I_p\omega\dot{\gamma}_x + (D_s + D_f)\dot{\gamma}_y - \left(D_s + \frac{1}{2}D_f\right)\omega\gamma_x + (K_s + K_f)\gamma_y = \gamma_s\left(K_f \sin\psi_s - \frac{1}{2}D_f\omega \cos\psi_s\right) + K_s\gamma_{ri}\sin\omega t \quad (1)$$

where I_t and I_p are the transverse and polar moments of inertia, respectively. Equations (1) are linear; therefore, solutions of γ_x and γ_y for the two forcing inputs, γ_s and γ_{ri}, can be superimposed. However, since γ_s is static, the corresponding rotor response is also static (Green, 1989). Inasmuch as this static response is important to the complete rotor response, it is not of interest in this dynamic investigation. Only the dynamic response to the forcing input, γ_{ri}, will be considered here. Although Eqs. (1) are particular to a rigid body FMR seal they are still useful for the current investigation. Their individual terms will reappear in the various complex extended transfer matrices.

Complex Extended Transfer Matrix Modeling

The size of a general transfer matrix for shaft free vibration problems is eight by eight (8 × 8) (Pestel and Leckie, 1963). Since the external force (dynamic load due to γ_{ri}) is sinusoidal having a frequency of the shaft speed, ω, a complex formulation is functional. To handle the external force, the size of the complex transfer matrix is extended to nine by nine (9 × 9). These make up the complex extended transfer matrix. Consequently, the state vector at station i, Z_i, is

$$Z_i = \{u_x, \theta_y, M_y, -V_x, -u_y, \theta_x, M_x, V_y, 1\}_i^T \quad (2)$$

where u, θ, M, and V are the complex magnitudes of deflection, slope, moment, and shear force, respectively, as shown in Fig.

Nomenclature

d = rotor center of mass axial offset
D_f = angular fluid film damping
D_s = angular support damping
EI = flexural rigidity of shaft
F_i = field matrix
I_t = transverse moment of inertia
I_p = polar moment of inertia
K_e = angular elastomeric O-ring stiffness
K_f = angular fluid film stiffness
K_s = angular support stiffness, $K_{sp} + K_e$
K_{sp} = angular spring stiffness
M_x, M_y = moments in the *xyz*-system
l = length of shaft section
P_i = point matrix
t = time
u_x, u_y = deflections in the *xyz*-system
U = overall transfer matrix
V_x, V_y = shear forces in the *xyz*-system
xyz = inertial system
Z = state vector
γ_{ri} = initial rotor misalignment
γ_{rI} = rotor angular response to γ_{ri}
γ_s = fixed stator misalignment
γ_x, γ_y = components of rotor angular response in the *xyz*-system
θ_x, θ_y = shaft section and rotor tilts (slopes) in the *xyz*-system
ϕ = phase angle of θ with respect to γ_{ri}
ψ = phase angle of γ_{rI} with respect to γ_{ri}
ψ_s = phase angle of γ_s with respect to the *x*-axis
ω = shaft speed

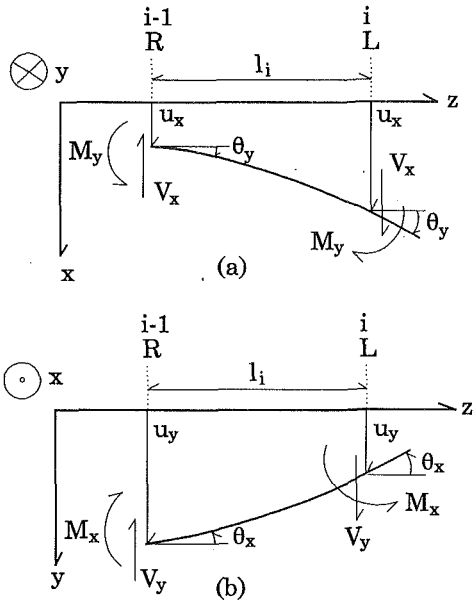

Fig. 3 Free body diagrams of section *i* in the *xz* and *yz* planes

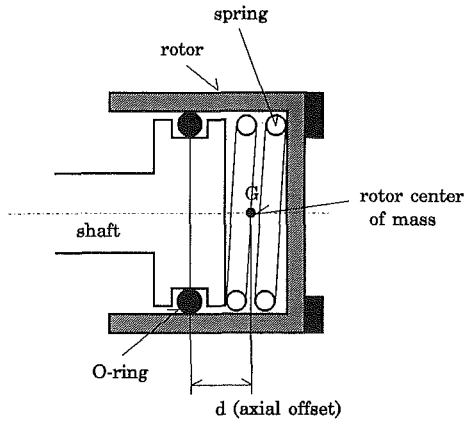

Fig. 4 Definition of axial offset of the rotor center of mass

3. The aforementioned are all functions of ω. The state vector at the left of station i, Z_i^L, is related to the state vector at the right of station $i-1$, Z_{i-1}^R, through the field matrix, F_i,

$$Z_i^L = F_i Z_{i-1}^R \tag{3}$$

The field matrix of a shaft section i, F_i, is defined as follows:

$$F_i = \begin{bmatrix} 1 & l & \frac{l^2}{2EI} & \frac{l^3}{6EI} & 0 & 0 & 0 & 0 & 0 \\ 0 & 1 & \frac{l}{EI} & \frac{l^2}{2EI} & 0 & 0 & 0 & 0 & 0 \\ 0 & 0 & 1 & l & 0 & 0 & 0 & 0 & 0 \\ 0 & 0 & 0 & 1 & 0 & 0 & 0 & 0 & 0 \\ 0 & 0 & 0 & 0 & 1 & l & \frac{l^2}{2EI} & \frac{l^3}{6EI} & 0 \\ 0 & 0 & 0 & 0 & 0 & 1 & \frac{l}{EI} & \frac{l}{2EI} & 0 \\ 0 & 0 & 0 & 0 & 0 & 0 & 1 & l & 0 \\ 0 & 0 & 0 & 0 & 0 & 0 & 0 & 1 & 0 \\ 0 & 0 & 0 & 0 & 0 & 0 & 0 & 0 & 1 \end{bmatrix}_i \quad i=1,2,3,4 \tag{4}$$

where EI and l are, respectively, the flexural rigidity and length of section i. Since the support angular stiffness and damping, K_s and D_s, are quantities that instigate forces resulting from relative motion between shaft and rotor (stations four and five in Fig. 2(*b*)), they are expressed in a separate field matrix. Assuming no relative radial motion between the shaft and the rotor (i.e., O-ring compression remains unchanged), the field matrix, F_5, is devised as follows:

$$F_5 = \begin{bmatrix} 1 & 0 & 0 & 0 & 0 & 0 & 0 & 0 & 0 \\ 0 & 1 & \frac{1}{K_s+jD_s\omega} & 0 & 0 & 0 & 0 & 0 & 0 \\ 0 & 0 & 1 & 0 & 0 & 0 & 0 & 0 & 0 \\ 0 & 0 & 0 & 1 & 0 & 0 & 0 & 0 & 0 \\ 0 & 0 & 0 & 0 & 1 & 0 & 0 & 0 & 0 \\ 0 & 0 & 0 & 0 & 0 & 1 & \frac{1}{K_s+jD_s\omega} & 0 & 0 \\ 0 & 0 & 0 & 0 & 0 & 0 & 1 & 0 & 0 \\ 0 & 0 & 0 & 0 & 0 & 0 & 0 & 1 & 0 \\ 0 & 0 & 0 & 0 & 0 & 0 & 0 & 0 & 1 \end{bmatrix} \tag{5}$$

The term $K_s + jD_s\omega$ is the angular complex impedance of the support caused by shear deformation. K_s and D_s for an elastomeric O-ring secondary seal are typically frequency dependent (Green and Etsion, 1986).

If there is an axial offset of the rotor center of mass from the pitch axis (represented by d in Fig. 4), its effect has to be included in a transfer matrix. The additional section generated by d is modeled as a massless rigid bar. The entire rotor mass is attached at one end of the bar while an angular spring and a damper (K_s and D_s) are attached at the other end. To construct the field matrix for this bar section, Eq. (4) is used with two modifications: First, l is replaced by d; and second, since the bar is assumed rigid then

$$\frac{d}{EI}, \quad \frac{d^2}{EI}, \quad \frac{d^3}{EI} \to 0 \tag{6}$$

Hence, the field matrix of the axial offset is

$$F_d = \begin{bmatrix} 1 & d & 0 & 0 & 0 & 0 & 0 & 0 & 0 \\ 0 & 1 & 0 & 0 & 0 & 0 & 0 & 0 & 0 \\ 0 & 0 & 1 & d & 0 & 0 & 0 & 0 & 0 \\ 0 & 0 & 0 & 1 & 0 & 0 & 0 & 0 & 0 \\ 0 & 0 & 0 & 0 & 1 & d & 0 & 0 & 0 \\ 0 & 0 & 0 & 0 & 0 & 1 & 0 & 0 & 0 \\ 0 & 0 & 0 & 0 & 0 & 0 & 1 & d & 0 \\ 0 & 0 & 0 & 0 & 0 & 0 & 0 & 1 & 0 \\ 0 & 0 & 0 & 0 & 0 & 0 & 0 & 0 & 1 \end{bmatrix} \tag{7}$$

In the case where no axial offset exists ($d = 0$), F_d is simply the identity matrix.

The state vector at the right of a lumped disk at station i, Z_i^R, is related to the state vector at the left of that lumped disk, Z_i^L, by a point matrix, P_i, such that

$$Z_i^R = P_i Z_i^L \tag{8}$$

The point matrix of a lumped shaft disk i, P_i, is devised as

$$P_i = \begin{bmatrix} 1 & 0 & 0 & 0 & 0 & 0 & 0 & 0 & 0 \\ 0 & 1 & 0 & 0 & 0 & 0 & 0 & 0 & 0 \\ 0 & -I_t\omega^2 & 1 & 0 & 0 & -jI_p\omega^2 & 0 & 0 & 0 \\ m\omega^2 & 0 & 0 & 1 & 0 & 0 & 0 & 0 & 0 \\ 0 & 0 & 0 & 0 & 1 & 0 & 0 & 0 & 0 \\ 0 & 0 & 0 & 0 & 0 & 1 & 0 & 0 & 0 \\ 0 & jI_p\omega^2 & 0 & 0 & 0 & -I_t\omega^2 & 1 & 0 & 0 \\ 0 & 0 & 0 & 0 & m\omega^2 & 0 & 0 & 1 & 0 \\ 0 & 0 & 0 & 0 & 0 & 0 & 0 & 0 & 1 \end{bmatrix}_i \quad i=1,2,3,4 \tag{9}$$

where the gyroscopic effect is expressed by $I_p\omega^2$. The fluid film angular stiffness and damping, K_f and D_f (Green, 1987), are quantities that instigate forces on the rotor due to its motion relative to an inertial stator, i.e., K_f and D_f are "absolute" quantities. Therefore, their effects are included in the point matrix that follows. The point matrix of disk five (i.e., the FMR), P_5, is obtained from Eqs. (1) as follows:

$$P_5 = \begin{bmatrix} 1 & 0 & 0 & 0 & 0 & 0 & 0 & 0 & 0 \\ 0 & 1 & 0 & 0 & 0 & 0 & 0 & 0 & 0 \\ 0 & K_f - I_t\omega^2 + jD_f\omega & 1 & 0 & 0 & -\frac{1}{2}D_f\omega - jI_p\omega^2 & 0 & 0 & jK_s\gamma_{ri} \\ m\omega^2 & 0 & 0 & 1 & 0 & 0 & 0 & 0 & 0 \\ 0 & 0 & 0 & 0 & 1 & 0 & 0 & 0 & 0 \\ 0 & 0 & 0 & 0 & 0 & 1 & 0 & 0 & 0 \\ 0 & \frac{1}{2}D_f\omega + jI_p\omega^2 & 0 & 0 & 0 & K_f - I_t\omega^2 + jD_f\omega & 1 & 0 & -K_s\gamma_{ri} \\ 0 & 0 & 0 & 0 & m\omega^2 & 0 & 0 & 1 & 0 \\ 0 & 0 & 0 & 0 & 0 & 0 & 0 & 0 & 1 \end{bmatrix}_5 \quad (10)$$

where $\cos(\omega t)$ and $\sin(\omega t)$ have been replaced by 1 and $-j$, respectively. Noteworthy is the presence of the forcing function, γ_{ri}, in the ninth column of the matrix P_5.

Equations (3) and (8) are combined to give the transfer matrix P_iF_i for section i, effectively transferring properties at station $i-1$ to station i. Hence,

$$Z_i^R = P_iF_iZ_{i-1}^R \quad (11)$$

Applying Eq. (11) successively, Z_5^R and Z_0 are related by

$$Z_5^R = UZ_0 \quad (12)$$

where U is the overall transfer matrix

$$U = P_5F_dF_5P_4F_4P_3F_3P_2F_2P_1F_1 \quad (13)$$

It is important to emphasize that all transfer matrices correspond to a state vector, Z, which contains angular as well as lateral degrees of freedom, θ and u, respectively (see Eq. (2)). The result U, whether obtained analytically or numerically, effectively couples all degrees of freedom.

Applying the boundary conditions at the two ends, i.e., no deflection and slope at station 0, and no shear force and moment at station 5, Eq. (12) reduces to

$$-\begin{Bmatrix} U_{39} \\ U_{49} \\ U_{79} \\ U_{89} \end{Bmatrix} = \begin{bmatrix} U_{33} & U_{34} & U_{37} & U_{38} \\ U_{43} & U_{44} & U_{47} & U_{48} \\ U_{73} & U_{74} & U_{77} & U_{78} \\ U_{83} & U_{84} & U_{87} & U_{88} \end{bmatrix} \begin{Bmatrix} M_y \\ -V_x \\ M_x \\ V_y \end{Bmatrix}_0 \quad (14)$$

where U_{ij} are known elements of U. Upon solving Eq. (14) for Z_0, the intermediate state vectors, Z_1, Z_2, Z_3, and Z_4, and the end vector Z_5 are found by using Eq. (11) recursively. That is, all degrees of freedom have been found at every section, where of particular interest are the angular responses, θ_x and θ_y. The outlined CETM method proposes a numerical solution at a given shaft speed, ω. This procedure can be looped through a desired spectrum of frequencies.

Results and Discussions

The numerical values for the various parameters which model the actual seal test rig are given in the Appendix. The magnitude of the angular response of the FMR mechanical face seal, θ, is found from the elements of Z_5. Hence,

$$\theta = |\theta_{x,5}| = |\theta_{y,5}| \quad (15)$$

where $\theta_{x,5}$ and $\theta_{y,5}$ are the tilts (slopes) about the x and y axes at station 5, respectively. The transmissibility is then calculated as θ/γ_{ri}. The phase angle is found from the respective arguments

$$\phi = \angle\theta_{x,5} = \angle\theta_{y,5} + \frac{\pi}{2} \quad (16)$$

The dynamic response of the FMR mechanical face seal only (disregarding shaft dynamics and axial offset) was obtained analytically by Green (1989) in terms of transmissibility

$$\frac{\gamma_{rI}}{\gamma_{ri}} = \frac{K_s}{\sqrt{[(I_p - I_t)\omega^2 + (K_s + K_f)]^2 + \left(\frac{1}{2}D_f\omega\right)^2}} \quad (17)$$

and phase

$$\psi = -\tan^{-1}\frac{\frac{1}{2}D_f\omega}{(I_p - I_t)\omega^2 + (K_s + K_f)} \quad (18)$$

where γ_{rI} is the rotor angular response to γ_{ri}, and ψ is the phase angle of γ_{rI} with respect to γ_{ri}.

Results obtained from the current CETM method are compared with those obtained from the analysis by Green (1989), in Fig. 5 for the transmissibility, and in Fig. 6 for the phase; both as functions of the shaft speed. The comparison reveals results that are practically identical, except for a spike that occurs in the CETM results about 42,000 rpm. The spike is attributed to the resonance of the system. This was verified by a finite element analysis of free vibration of the shaft and rotor, which gave a first natural frequency about 42,000 rpm. In Fig. 5, the transmissibility increases in a limited range of ω (up to about 1200 rpm) because of the stiffness hardening of the O-ring. However, as ω increases above 1200 rpm, the transmissibility decreases monotonically because of the gy-

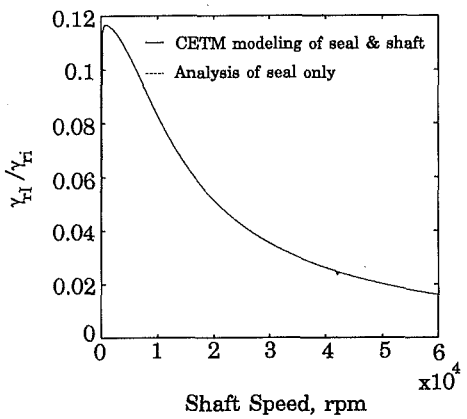

Fig. 5 Transmissibility versus shaft speed; comparison of CETM and analysis

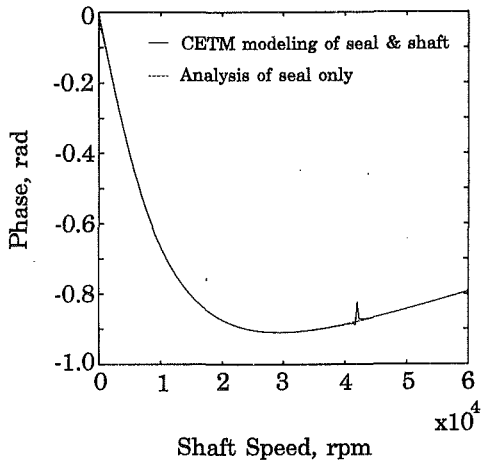

Fig. 6 Phase versus shaft speed; comparison of CETM and analysis

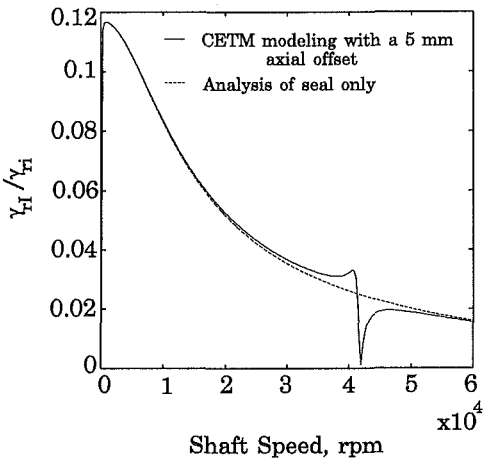

Fig. 7 Transmissibility versus shaft speed; FMR seal having 5 mm axial offset

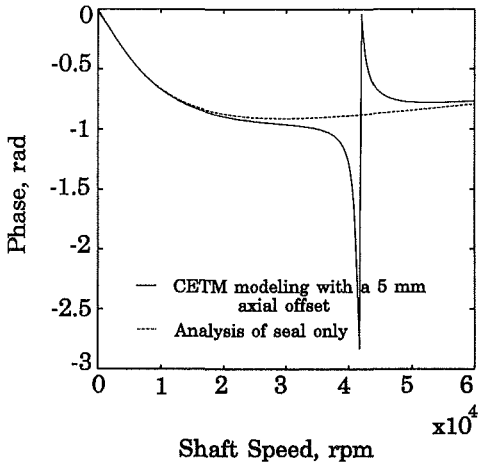

Fig. 8 Phase versus shaft speed; FMR seal having 5 mm axial offset

roscopic effect that overcomes the stiffness hardening of the O-ring (see Eq. (17) and the Appendix for K_s).

Since in any practical system it is impossible to entirely eliminate the axial offset of the rotor center of mass from the pitch axis, it is important to estimate its effect. Results obtained by the CETM method for an FMR having an estimated 5 mm axial offset, are shown in Fig. 7 for the transmissibility, and in Fig. 8 for the phase. The results provide evidence that the

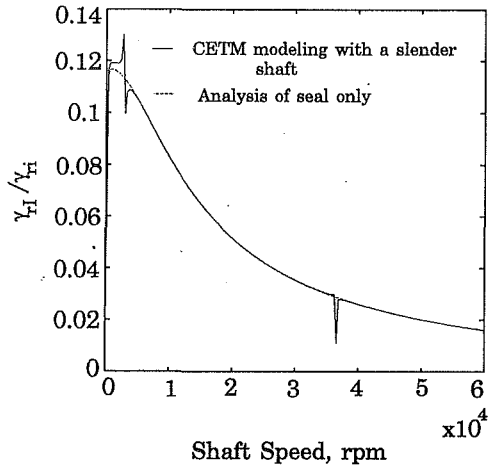

Fig. 9 Transmissibility versus shaft speed; slender shaft

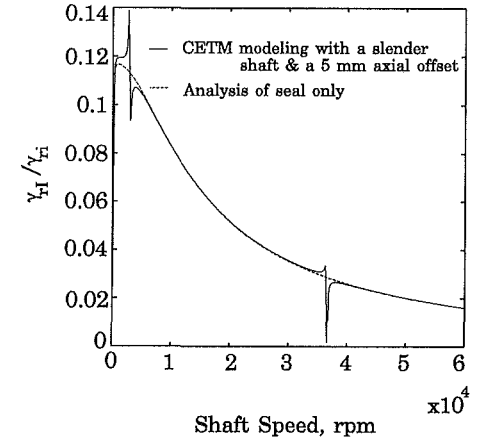

Fig. 10 Transmissibility versus shaft speed; slender shaft and 5 mm axial offset

shaft dynamics affects the seal dynamics at a range of ω from about 20,000 rpm to 60,000 rpm, where the response is most pronounced at resonance. In high speed turbomachinery this behavior must be confronted with. (In the test rig under consideration this effect is inconsequential because the maximum operating speed was designed to be less than 6000 rpm.)

To investigate the consequences of the shaft slenderness, the length of each shaft section is theoretically elongated three times without increasing its mass. Thus, the flexural rigidity is reduced by a factor of one-ninth. The transmissibility obtained by the CETM with the slender shaft is shown in Fig. 9. Two resonances are observed at 3000 rpm and 37,000 rpm, respectively. The first natural frequency is now considerably lower (most of rotating machinery in processing plant applications, for example, operate between 750 rpm to 15,000 rpm (Laws, 1987)). Even the second natural frequency is lower than the first natural frequency of the system with the original stiffer shaft. Consequently, the dynamic response of the FMR seal is severely affected by the shaft dynamics in operation under 6000 rpm. The transmissibility obtained by the CETM with the slender shaft and an additional 5 mm axial offset is shown in Fig. 10. The results show again an even more pronounced response at the first two resonances. The obvious conclusion is that the smaller the axial offset and the stiffer the shaft the better; practically, however, these may not be feasible.

Conclusions

The complex extended transfer matrix (CETM) method was formulated to solve the coupled problem of the dynamics of

the shaft and a noncontacting FMR mechanical face seal. The method was then applied to analyze an actual test rig. The results from the CETM method were compared to results of a closed-form solution of an FMR seal, a solution that was limited to rigid body dynamics (i.e., did not include shaft flexibility or axial offset of the rotor center of mass).

The results show that when a seal is being driven by a slender shaft, the seal dynamics is greatly affected by the shaft dynamics even at relatively low operating speeds. This particularly holds in high speed applications. The flexibility of the shaft and the axial offset of the rotor center of mass were found to have an adverse effect on the dynamic behavior of a seal, where the latter enhances the response at resonance.

In the test rig under consideration the driving shaft was especially designed to be very stiff, therefore, its effect on the dynamic response of the seal was negligible in the designed speed range. Here the CETM method and the closed-form solution produced practically identical results. In general seal applications, however, the closed-form solution may not realistically predict the seal dynamic response.

The CETM method established here offers a complete dynamic analysis of a seal tribosystem including the effects of the shaft, fluid film, secondary seal, flexibly mounted rotating element, and axial offset. The method is modular and can accommodate other triboelements such as bearings, gears, and the like, to provide comprehensive analysis of elaborate tribosystems.

Acknowledgment

This work was supported in part by the National Science Foundation under grant Number MSM-8619190. This support is gratefully acknowledged.

References

Etsion, I., 1982, "A Review of Mechanical Face Seal Dynamics," *The Shock and Vibration Digest*, Vol. 14, No. 4, pp. 9–14.

Etsion, I., 1985, "Mechanical Face Seal Dynamics Update," *The Shock and Vibration Digest*, Vol. 17, No. 4, pp. 11–15.

Etsion, I., 1991, "Mechanical Face Seal Dynamics 1985–1989," *The Shock and Vibration Digest*, Vol. 23, No. 4, pp. 3–7.

Green, I., and Etsion, I., 1985, "Stability Threshold and Steady-State Response of Noncontacting Coned-Face Seals," *ASLE Trans.*, Vol. 28, No. 4, pp. 449–460.

Green, I., and Etsion, I., 1986, "Pressure and Squeeze Effects on the Dynamic Characteristics of Elastomer O-Rings Under Small Reciprocating Motion," ASME JOURNAL OF TRIBOLOGY, Vol. 108, No. 3, pp. 439–445.

Green, I., 1987, "The Rotor Dynamic Coefficients of Coned-Face Mechanical Seals with Inward or Outward Flow," ASME JOURNAL OF TRIBOLOGY, Vol. 109, No. 1, pp. 129–135.

Green, I., 1989, "Gyroscopic and Support Effects on the Steady-State Response of a Noncontacting Flexibly Mounted Rotor Mechanical Face Seal," ASME JOURNAL OF TRIBOLOGY, Vol. 111, pp. 200–208.

Green, I., 1990, "Gyroscopic and Damping Effects on the Stability of a Noncontacting Flexibly-Mounted Rotor Mechanical Face Seal," *Dynamics of Rotating Machinery*, Hemisphere Publishing Company, pp. 153–173.

Laws, C. W., 1987, "Vibration Condition Monitoring of Rotating Machinery," *Institution of Mechanical Engineers*, C120/87, pp. 15–26.

Lee, A. S., and Green, I., 1992, "Higher Harmonic Oscillation in a Flexibly Mounted Rotor Mechanical Seal Test Rig," ASME, Proceedings of Friction-Induced Vibration, Chatter, Squeal, and Chaos, Winter Annual Meeting, Anaheim, CA (November 1992), DE-Vol. 49, 157–164. To appear in ASME *Journal of Vibration and Acoustics*.

Lee, A. S., 1992, "An Experimental Investigation of a Noncontacting Flexibly Mounted Rotor Mechanical Face Seal," Ph.D. thesis, Georgia Institute of Technology, Mar.

Marscher, W. D., 1987, "Relationship Between Pump Rotor System Tribology and Appropriate Vibration Specifications for Centrifugal Pumps," Institute of Mechanical Engineers, I Mech E Conference Publication, London, England, pp. 157–167.

Myklestad, N. O., 1944, "A New Method of Calculating Natural Modes of Uncoupled Bending Vibration of Airplane Wings and Other Types of Beams," *Journal of the Aeronautical Sciences*, pp. 153–162.

Pestel, E. C., and Leckie, F. A., 1963, *Matrix Methods in Elasto Mechanics*, McGraw-Hill, New York, NY.

Prohl, M. A., 1945, "A General Method for Calculating Critical Speeds of Flexible Rotors," ASME *Journal of Applied Mechanics*, pp. A142–A148.

Rao, J. S., 1983, *Rotor Dynamics*, Wiley.

Salant, R. F., and Blasbalg, D. A., 1991, "Dynamic Behavior of Two-Phase Mechanical Face Seals," *STLE Tribology Trans.*, Vol. 34, No. 1, pp. 122–130.

Yasuna, J. A., and Hughes, W. F., 1992, "Squeeze Film Dynamics of Two-Phase Seals," ASME JOURNAL OF TRIBOLOGY, Vol. 114, No. 2, pp. 236–246.

APPENDIX

The numerical values for the various parameters of the actual test rig (Lee and Green, 1992) are

EI	$= 1338.2\ \text{Pa}\cdot\text{m}^4$	d	$= 0.005\ \text{m}$
I_{p1}	$= 3.2847\times10^{-6}\ \text{kg}\cdot\text{m}^2$	I_{p2}	$= 2.4447\times10^{-5}\ \text{kg}\cdot\text{m}^2$
I_{p3}	$= 2.5027\times10^{-6}\ \text{kg}\cdot\text{m}^2$	I_{p4}	$= 2.0652\times10^{-5}\ \text{kg}\cdot\text{m}^2$
I_{p5}	$= 4.1619\times10^{-4}\ \text{kg}\cdot\text{m}^2$	I_{t1}	$= 8.3497\times10^{-6}\ \text{kg}\cdot\text{m}^2$
I_{t2}	$= 1.2513\times10^{-5}\ \text{kg}\cdot\text{m}^2$	I_{t3}	$= 4.2175\times10^{-6}\ \text{kg}\cdot\text{m}^2$
I_{t4}	$= 1.0829\times10^{-5}\ \text{kg}\cdot\text{m}^2$	I_{t5}	$= 2.8032\times10^{-4}\ \text{kg}\cdot\text{m}^2$
l_1	$= 0.01667\ \text{m}$	l_2	$= 0.01984\ \text{m}$
l_3	$= 0.01588\ \text{m}$	l_4	$= 0.01667\ \text{m}$
m_1	$= 0.07241\ \text{kg}$	m_2	$= 0.08621\ \text{kg}$
m_3	$= 0.05517\ \text{kg}$	m_4	$= 0.08803\ \text{kg}$
m_5	$= 0.5198\ \text{kg}$	γ_{ri}	$= 4\times10^{-4}\ \text{rad}$
K_f	$= 1134.5\ \text{N}\cdot\text{m/rad}$	K_s	$= 5.35 + 146.1\ \omega^2/(36.36+\omega^2)\ \text{N}\cdot\text{m/rad}$
D_f	$= 2.1476\ \text{N}\cdot\text{m}\cdot\text{s/rad}$	D_s	$= 881.4/(36.36+\omega^2)\ \text{N}\cdot\text{m}\cdot\text{s/rad}$

The dependency of K_s and D_s upon frequency was obtained from experiments done on a support consisting of a spring and two Buna-N O-rings (Lee, 1992). The fluid film coefficients K_f and D_f were calculated for water pressure of 0.283 MPa and viscosity of 0.89 mPa·s. The rotor input forcing misalignment, $\gamma_{ri} = 0.4$ mrad, is in the bulk of measurements. (The numerical value of the latter is actually insignificant because results are presented in a transmissibility form, i.e., ratio of output to input.) The various lumped masses and moments of inertia were calculated based upon the geometry of the shaft and the rotor, and upon the length of section i (the mass of the spring, however small, is lumped into the mass of the rotor). The index $i = 1$ to 4 corresponds to the shaft, and $i = 5$ represents the rotor. EI is the flexural rigidity of the shaft, and $d = 5$ mm is a generous estimate of the center of mass axial offset.